LETTER

Design and Fabrication of Bimetallic Colloidal "Janus" Particles

Shengrong Ye and R. Lloyd Carroll*

C. Eugene Bennett Department of Chemistry, West Virginia University, Morgantown, West Virginia 26506

ABSTRACT In this work, we demonstrate the results of a novel approach developed in our lab to prepare bimetallic Janus particles, which are composed of silica particles with differing metals on opposite hemispheres. SEM imaging, EDS mapping, and XPS analysis clearly indicate that beads are capped with two different metals, typically leaving an equatorial belt around the particle composed of uncoated silica. Oxidation of some metal components can be induced by oxygen plasma exposure, producing compositional and morphological changes. The facile conversion of metal to metal oxide heralds a wide variety of Janus particles with different electronic, optical, and magnetic properties.

KEYWORDS: Janus particles • bimetallic • e-beam evaporation • chemical transformation

INTRODUCTION

"Janus" particles (1) (that is, particles having two different materials on opposite faces) have a wide range of potential applications in drug delivery, microfluidic systems, optical biosensors, and electronic devices (2–7). A primary feature of all Janus particles is anisotropy, whether due to chemically or morphologically asymmetric structure. Availability of two or more different materials in one single unit would allow varied physical or chemical functionalities. Structurally, Janus particles may be considered as unique building blocks to prepare advanced ordered structures based upon their anisotropic attributes (8–13). In addition, the surface multifunctionality of Janus particles provides potential uses in surface assembly and cargo transport. Of particular interest is recent work demonstrating that Pt-silica asymmetric particles and bimetallic nanorods undergo autonomous motion due to conversion of stored chemical energy to mechanical movement without external intervention, which is very promising for driving micro- or nanobased devices (14–16). One of the driving forces behind our research on bimetallic Janus particles was to produce analogous spherical materials.

Currently, there are many methods to prepare a wide range of Janus particles for varied purposes (2, 17–40). In this work, we will demonstrate the results of a novel approach developed in our laboratory to prepare bimetallic Janus particles, comprising silica particles with different metals on opposite hemispheres. These bimetallic Janus particles have been thoroughly characterized by scanning electron microscopy (SEM) and energy dispersive X-ray spectroscopy (EDS), which indicate that all silica beads are capped with two different metals, typically leaving an equatorial belt around the particle composed of uncoated silica. Subsequent possible chemical modification and transformation of these bimetallic Janus particles would provide increased functionality. For instance, metals on the Janus particle can be transformed by heterogeneous phase reactions to form other species. This transition is expected to lead to a wide variety of Janus particles with different electronic, optical, and magnetic properties.

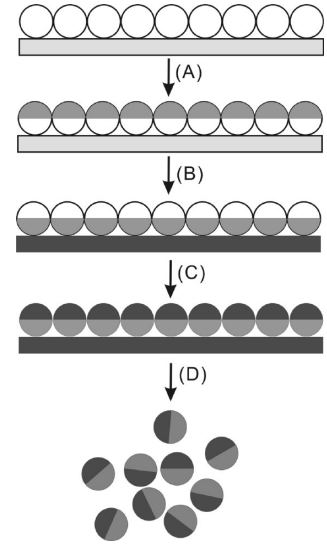

FIGURE 1. Schematic strategy to create bimetallic Janus particles: (A) metal evaporation; (B) inversion; (C) metal evaporation; (D) dispersion.

RESULTS AND DISCUSSION

A schematic representation of our four-step approach to fabricate the bimetallic Janus particles is summarized in Figure 1. A single layer of self-assembled silica beads are coated with one metal using e-beam evaporation. The beads are then inverted, and coated with another metal. Finally, the formed bimetallic Janus particles are dispersed in solution by sonication. As shown in Figure 2a, metal evaporation caused no apparent damage to the packing of the beads. Note that "shadows" formed underneath the spheres during the process of e-beam evaporation (Figure 2b). In contrast

* Corresponding author. E-mail: lloyd.carroll@mail.wvu.edu.
Received for review November 29, 2009 and accepted February 15, 2010
DOI: 10.1021/am900839w

Published on Web 02/22/2010

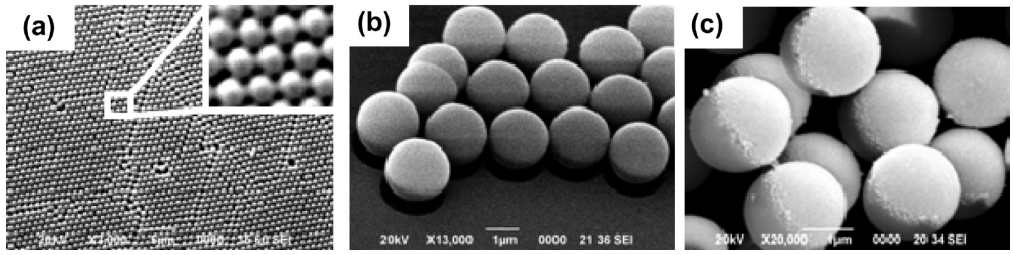

FIGURE 2. SEM images are shown of (a) hexagonally packed silica beads after first metal evaporation of gold with titanium as adhesion layer (inset shows higher magnification view of the layer); (b) half-gold-coated silica beads on a 40°-tilted sample stage; (c) individual half-gold-coated silica beads. Scale bar (a) 5, (b) 1, and (c) 1 μm.

to metal deposition by sputter coating, e-beam evaporation is a ballistic process, in which atoms emitted from the source crucible travel in straight lines in vacuum and uniformly coat the metal in a line-of-sight fashion onto beads, producing a "shadow" of metal on the substrate. In addition, only the top surface of the particle is coated with a thick layer of metal - because of the bead curvature, the metal thickness decreases as the "equator" of the bead is approached. Clear phase boundaries visible by SEM imaging easily differentiate the metal hemisphere from the silica (Figure 2c).

An important requirement for successful fabrication of double-faced Janus particles was the identification of an appropriate adhesive substrate used to "flip" the beads. Three criteria were considered: adhesion to beads, heat tolerance, and release characteristics. Adhesion to beads should be sufficient to pick up the submicrometer structure and hold them securely, but should not have a permanent effect on the metal already evaporated on the surface. The second evaporation of metal occurs with beads stuck on the adhesive substrate, so it must tolerate temperatures up to 150 °C (as measured inside the e-beam evaporation chamber during evaporation). Release characteristics were important in that an adhesive that did not release the beads would render them useless, and if the adhesive material remained adsorbed to the beads, it would interfere with the desired properties, either by occluding the surface or adhering beads together. Ideally, the adhesive should be completely soluble in solvent or removable by other processes, leaving uncontaminated Janus particles. Many adhesive substrates were tried, including commercial double-sided tapes, carbon tape used as a conductive adhesive for samples in SEM, epoxies, and sparingly cross-linked polydimethylsiloxane. The best substrate we have identified to invert the beads was the commercially available double-sided adhesive copper tape, commonly used as a conductive adhesive for SEM substrates or EM shielding applications. More than 90% of the beads on a substrate can be picked up by a single application of the copper tape. As shown in Figure 3, the inversion process had no obvious effect on the packing of the beads. The copper tape adhesive is tolerant of the elevated temperature, showing no deformation or distortion over long periods of e-beam evaporation. Importantly, the acrylic adhesive on the tape is very soluble in acetone, providing a facile route to remove the beads from the substrate. Simple sonication in a solution of acetone releases the beads, and solvent washing with acetone produces Janus particles with no trace of adhesive adsorbed, as indicated

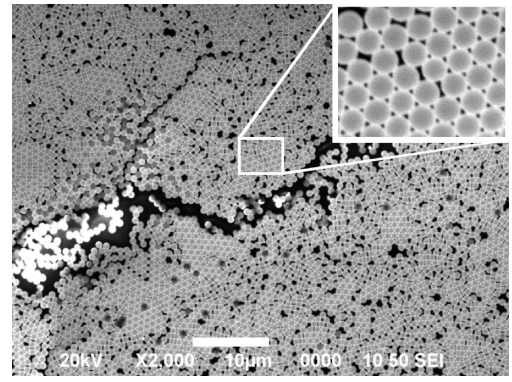

FIGURE 3. Half-gold-coated silica beads inverted on the copper tape followed by evaporation of 20 nm thick platinum (inset shows higher magnification view of the layer). Scale bar 10 μm.

by IR and XPS spectroscopy (see Figures S1 and S2 in the Supporting Information).

Silica beads of sizes ranging from 800 nm to 4 μm in diameter have been successfully inverted and evaporated with two different metals. Initial expectations were that the silica beads would be fully covered by two metals, one on each side, with an overlap or contact between the metals at the equatorial ring around the particles. However, as described above, the deposited metal thins as the equatorial region of the bead is approached. With metals deposited on both sides, both thin to nonexistence at the equator, leaving an uncoated belt of silica on each bimetallic Janus particle. EDS mapping verified this result, demonstrating that the metals do not fully coat on the bead hemisphere. Figure 4 shows a typical SEM image and EDS mapping result of those Au/Pt bimetallic Janus particles that are made with our approach. Note, as indicated in Figure 4a, that the edge of Au tends to be smooth and extends to the equator whereas the edge of Pt remains sharp, and the size of metal "cap" is smaller. The difference is due to the presence of Ti as an adhesion layer between the Au and silica. Ti and Cr are commonly used as adhesion promoters for noble metals because they adhere more uniformly to silica substrates than Au and Pt. We have found that the addition of Ti as an adhesion layer for Pt on silica also improved the wettability of Pt (data not shown), and thus narrowed the belt gap between two capping metals. To further understand the interfacial interaction between metals and the silica substrate, we are currently investigating the effect of metal deposition rate, local temperature at the substrate surface during deposition, curvature of the surface, and the effect

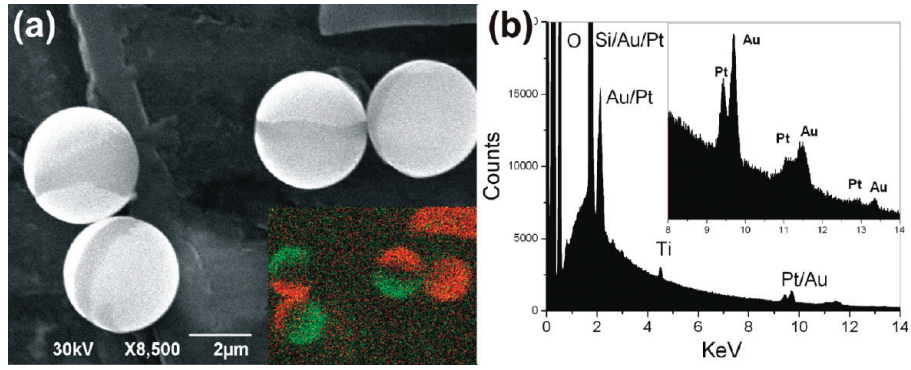

FIGURE 4. SEM image and EDS mapping results for 4 μm Au/Pt bimetallic Janus particles (Ti as adhesion layer between Au and SiO_2); (a) secondary electron image, inset: EDS mapping indicating Au (green) and Pt (red); (b) X-ray energy-dispersive spectrum, inset: enlarged region of the XPS trace. Scale bar 2 μm.

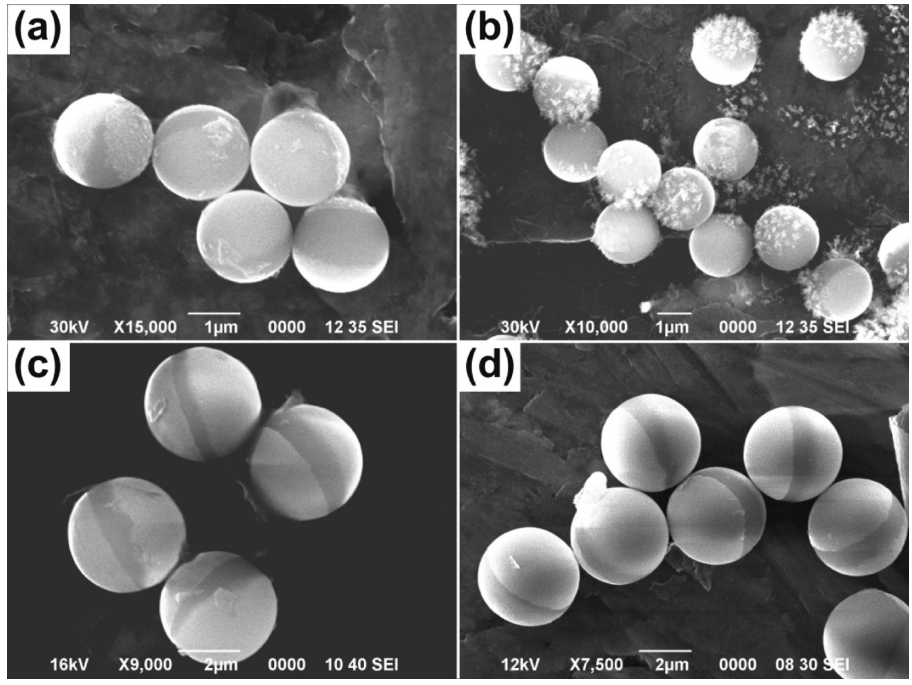

FIGURE 5. SEM images of 2 μm Au/Ag bimetallic Janus particles (a) before and (b) after oxygen plasma exposure and 4 μm Au/Ni bimetallic Janus particles (c) before and (d) after oxygen plasma exposure. Scale bar (a, b) 1 and (c, d) 2 μm.

of surface chemistry on the total coverage of the metal on the silica particles.

This approach through e-beam evaporation seems to be generally applicable for any metal which can be deposited by evaporation. Through this approach, a broad variety of metals, including ferrous metals, reactive metals, and noble metals have been used to fabricate various combinations of bimetallic Janus particles. Analysis of the resulting particles by SEM and EDS clearly indicates the presence of two metals, one at each hemisphere of the silica beads with uncoated equatorial silica belts. An example of SEM imaging and EDS mapping for Co/Ni bimetallic Janus particles is shown in Figure S3 in the Supporting Information.

A potential advantage of these bimetallic systems is that selective chemical modification of each of the metals and the silica belt can facilitate multifunctional materials. Possible modifications include chemical adsorption, formation of self-assembled monolayers, covalent coupling, and chemical transformation of metals into other materials. Here, we have demonstrated the transformation of metal surfaces to metal oxides through direct exposure of the Janus particles to oxygen plasma. Because of their ease of oxidation, thin films of Ag, Ni, Co, and Al are susceptible to air oxidation, and in some cases spontaneously transform, at least in part, into corresponding metal oxides. Direct heterogeneous oxidation reactions have been performed by exposing bimetallic Janus particles to RF-generated air-oxygen plasma in a plasma cleaning system for several minutes. The metal oxides are marked by changes in composition, but also by changes in morphology and structure. For example, SEM images a and b shown in Figure 5 demonstrate the transformation and corresponding morphological change of Ag to Ag_2O on Ag/Au bimetallic Janus particles before and after plasma exposure, respectively. Ni/Au bimetallic Janus particles, however, do not show any significant change in morphology upon exposure to oxidation (Figure 5c,d). Characterization by XPS of silver and nickel films (20 nm) on a flat silicon substrate (as a model system of comparison to

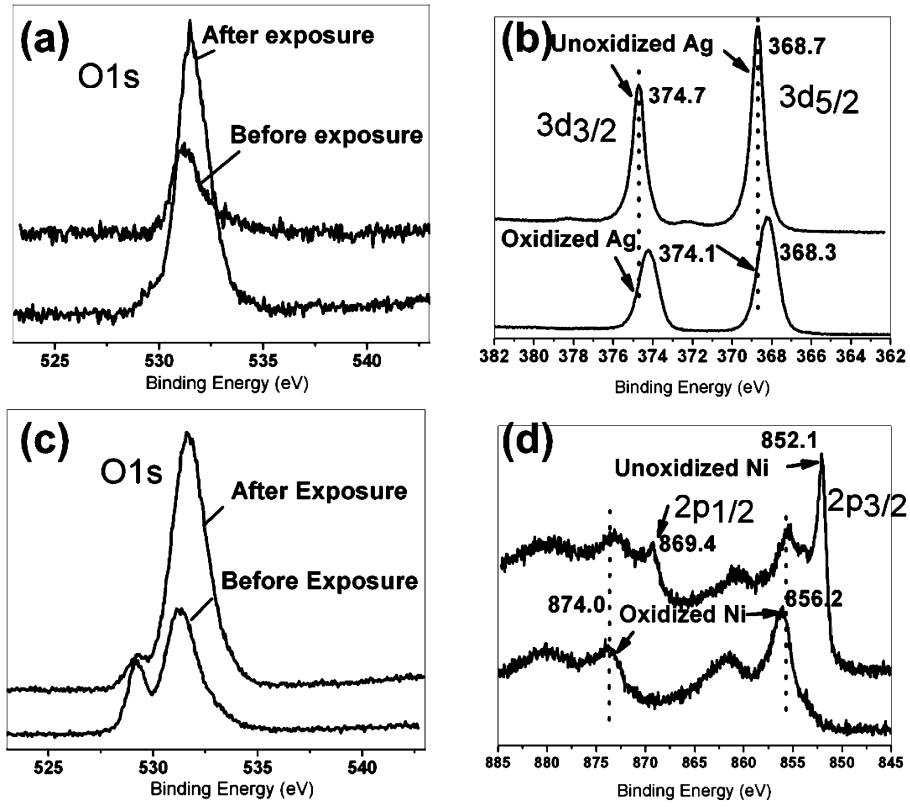

FIGURE 6. XPS patterns of thin film (a, b) Ag and (c, d) Ni on Si (111) after oxygen plasma exposure.

the Janus particles) exposed to oxygen plasma clearly indicates the oxidation reaction due to the presence of an intensified oxygen peak and the shift of metal peaks (Figure 6), which indicates the change in the oxidation state of the metal. Note that the model system is necessary for comparison because the XPS data was convoluted by the random orientation of the bimetallic Janus particle. Furthermore, the SEM images also verify the similar morphological change in both Ag and Ni thin films on the flat surface, compared to the same films on the bimetallic Janus particle.

In summary, a simple approach has been applied for the first time to fabricate bimetallic Janus particles, which comprise colloidal spherical silica beads, capped with various metals on opposite faces, leaving an equatorial silica belt around the particle. Chemical transformation can be achieved simply by heterogeneous oxidation reaction to form other types of Janus particles for more valuable usages. The presence of the uncoated silica belt also provides an opportunity to assemble various useful functionalities. Through these and other approaches, the bimetallic Janus particle is expected to have applications in a variety of fields, such as photochemistry, photocatalysis, device photonics, and novel magnetic and semiconductor materials.

EXPERIMENTAL SECTION

Fabrication of Bimetallic Janus Particles. A typical approach to make bimetallic Janus particles using e-beam vacuum evaporation is described as below. Uniform silica submicro- and microspheres were purchased from Bangs Laboratories, Inc. As an initial support, glass substrates were treated with piranha solution (H_2O_2:H_2SO_4 = 1:3) to form a hydrophilic surface. The substrates were immersed in the piranha solution for 30 min, then rinsed with DI water, and finally dried in a stream of dry nitrogen. After drying, delivery of a drop (~20 μL) of a suspension of beads (~1 % solids) to the surface produced a predominately close-packed monolayer of beads on the glass substrate. The self-assembled beads were first coated with one selected metal and then adhered to an adhesive support and inverted, followed by evaporation of a thin film of another metal. Finally, the beads were released from the support by sonication in acetone, washed with acetone three times, and resuspended in water. Various combinations of different metals have been successfully deposited on opposite sides of the silica beads to form bimetallic Janus particles. Metals that have been used include gold, platinum, silver, nickel, cobalt, and aluminum. Titanium was added as intermediate adhesion layer between gold and silica—other metals were used with no adhesion layer. For instance, 4 μm Au/Pt bimetallic Janus particles were produced by evaporation of 5 nm Ti and 20 nm Au on one side and then 20 nm Pt on the other. Metal evaporation was performed in an electron-beam evaporator (Temescal BJD-2000). SEM (JEOL JSM-6490LV) was used to image the particles at each step of the procedure. An EDS detector coupled with SEM was used for elemental analysis. XPS (Phi 5000 Versaprobe) was used to characterize the oxidation state of metals after oxygen plasma exposure.

Acknowledgment. This work was supported by the National Science Foundation (grant #EPS-0554328) and the WVNano Initiative at WVU. We gratefully acknowledge Yuan Li and Andy Woodworth for assistance with XPS, and Keith Morris and the WVU Forensic Science Program for access to SEM-EDS resources.

Supporting Information Available: Figure S1 shows comparative FTIR traces of the beads and adhesive tape demonstrating complete removal of the adhesive from the

Janus particles. Figure S2 shows high-resolution XPS of the C1s region of beads before exposure to adhesive, after exposure and purposefully incomplete rinsing, and after complete rinsing. Figure S3 shows the SEM imaging and EDS mapping results for 4 μm Co/Ni bimetallic Janus particles (PDF). This material is available free of charge via the Internet at http://pubs.acs.org.

REFERENCES AND NOTES

(1) Casagrande, C.; Fabre, P.; Raphael, E.; Veyssie, M. *Europhys. Lett.* **1989**, *9*, 251–255.
(2) Walther, A.; Muller, A. H. E. *Soft Matter* **2008**, *4*, 663–668.
(3) Ozin, G. A.; Manners, I.; Fournier-Bidoz, S.; Arsenault, A. *Adv. Mater.* **2005**, *17*, 3011–3018.
(4) Sundararajan, S.; Lammert, P. E.; Zudans, A. W.; Crespi, V. H.; Sen, A. *Nano Lett.* **2008**, *8*, 1271–1276.
(5) Wang, J. *ACS Nano* **2009**, *3*, 4–9.
(6) Nisisako, T.; Torii, T.; Takahashi, T.; Takizawa, Y. *Adv. Mater.* **2006**, *18*, 1152–1156.
(7) Anker, J. N.; Behrend, C. J.; Huang, H.; Kopelman, R. *J. Magn. Magn. Mater.* **2005**, *293*, 655–662.
(8) Walther, A.; Drechsler, M.; Rosenfeldt, S.; Harnau, L.; Ballauff, M.; Abetz, V.; Muller, A. H. E. *J. Am. Chem. Soc.* **2009**, *131*, 4720–4728.
(9) Smoukov, S. K.; Gangwal, S.; Marquez, M.; Velev, O. D. *Soft Matter* **2009**, *5*, 1285–1292.
(10) Gangwal, S.; Cayre, O. J.; Velev, O. D. *Langmuir* **2008**, *24*, 13312–13320.
(11) Glotzer, S. C.; Solomon, M. J. *Nat. Mater.* **2007**, *6*, 557–562.
(12) Hong, L.; Cacciuto, A.; Luijten, E.; Granick, S. *Nano Lett.* **2006**, *6*, 2510–2514.
(13) Zhang, Z.; Glotzer, S. C. *Nano Lett.* **2004**, *4*, 1407–1413.
(14) Paxton, W. F.; Kistler, K. C.; Olmeda, C. C.; Sen, A.; St. Angelo, S. K.; Cao, Y.; Mallouk, T. E.; Lammert, P. E.; Crespi, V. H. *J. Am. Chem. Soc.* **2004**, *126*, 13424–13431.
(15) Fournier-Bidoz, S.; Arsenault, A. C.; Manners, I.; Ozin, G. A. *Chem. Comm.* **2005**, 441–443.
(16) Jonathan, R. H.; Richard, A. L. J.; Anthony, J. R.; Tim, G.; Reza, V.; Ramin, G. *Phy. Rev. Lett.* **2007**, *99*, 048102.
(17) Perro, A.; Reculusa, S.; Ravaine, S.; Bourgeat-Lami, E.; Duguet, E. *J. Mater. Chem.* **2005**, *15*, 3745–3760.
(18) Jiang, S.; Schultz, M. J.; Chen, Q.; Moore, J. S.; Granick, S. *Langmuir* **2008**, *24*, 10073–10077.
(19) Ho, C. C.; Chen, W. S.; Shie, T. Y.; Lin, J. N.; Kuo, C. *Langmuir* **2008**, *24*, 5663–5666.
(20) Ahmad, H.; Saito, N.; Kagawa, Y.; Okubo, M. *Langmuir* **2008**, *24*, 688–691.
(21) Walther, A.; Andre, X.; Drechsler, M.; Abetz, V.; Muller, A. H. E. *J. Am. Chem. Soc.* **2007**, *129*, 6187–6198.
(22) Dendukuri, D.; Hatton, T. A.; Doyle, P. S. *Langmuir* **2007**, *23*, 4669–4674.
(23) Nie, L.; Liu, S.; Shen, W.; Chen, D.; Jiang, M. *Angew. Chem., Int. Ed.* **2007**, *119*, 6437–6440.
(24) Dendukuri, D. P.; Daniel, C.; Collins, J.; Hatton, T. A.; Doyle, P. S. *Nat. Mater.* **2006**, *5*, 365–369.
(25) Nie, Z.; Li, W.; Seo, M.; Xu, S.; Kumacheva, E. *J. Am. Chem. Soc.* **2006**, *128*, 9408–9412.
(26) Suzuki, D.; Kawaguchi, H. *Colloid Polym. Sci.* **2006**, *284*, 1471–1476.
(27) Roh, K. H.; Martin, D. C.; Lahann, J. *Nat. Mater.* **2005**, *4*, 759–763.
(28) Takei, H.; Shimizu, N. *Langmuir* **1997**, *13*, 1865–1868.
(29) Fujimoto, K.; Nakahama, K.; Shidara, M.; Kawaguchi, H. *Langmuir* **1999**, *15*, 4630–4635.
(30) Erhardt, R.; Boker, A.; Zettl, H.; Kaya, H.; Pyckhout-Hintzen, W.; Krausch, G.; Abetz, V.; Muller, A. H. E. *Macromolecules* **2001**, *34*, 1069–1075.
(31) Cayre, O.; Paunov, V. N.; Velev, O. D. *Chem. Commun.* **2003**, 2296–2297.
(32) Cayre, O.; Paunov, V. N.; Velev, O. D. *J. Mater. Chem.* **2003**, *13*, 2445–2450.
(33) Erhardt, R.; Zhang, M.; Boker, A.; Zettl, H.; Abetz, C.; Frederik, P.; Krausch, G.; Abetz, V.; Muller, A. H. E. *J. Am. Chem. Soc.* **2003**, *125*, 3260–3267.
(34) Lu, Y.; Xiong, H.; Jiang, X.; Xia, Y.; Prentiss, M.; Whitesides, G. M. *J. Am. Chem. Soc.* **2003**, *125*, 12724–12725.
(35) Paunov, V. N.; Cayre, O. J. *Adv. Mater.* **2004**, *16*, 788–791.
(36) Du, Y. Z.; Tomohiro, T.; Zhang, G.; Nakamura, K.; Kodaka, M. *Chem. Commun.* **2004**, 616–617.
(37) Perro, A.; Reculusa, S.; Pereira, F.; Delville, M. H.; Mingotaud, C.; Duguet, E.; Bourgeat-Lami, E.; Ravaine, S. *Chem. Comm.* **2005**, 5542–5543.
(38) Gu, H.; Yang, Z.; Gao, J.; Chang, C. K.; Xu, B. *J. Am. Chem. Soc.* **2005**, *127*, 34–35.
(39) Takahara, Y. K.; Ikeda, S.; Ishino, S.; Tachi, K.; Ikeue, K.; Sakata, T.; Hasegawa, T.; Mori, H.; Matsumura, M.; Ohtani, B. *J. Am. Chem. Soc.* **2005**, *127*, 6271–6275.
(40) Pawar, A. B.; Kretzschmar, I. *Langmuir* **2009**, *25*, 9057–9063.

AM900839W